arXiv:1411.0713v1 [physics.chem-ph] 31 Oct 2014

Delocalized Quantum States Enhance Photocell Efficiency

Yiteng Zhang,[1,2] Sangchul Oh,[1] Fahhad H. Alharbi,[1] Greg Engel,[3] and Sabre Kais[1,2,*]

[1] *Qatar Environment and Energy Research Institute, Qatar Foundation, Doha, Qatar*
[2] *Department of Chemistry, Physics and Birck Nanotechnology Center, Purdue University, West Lafayette, IN 47907 USA*
[3] *Department of Chemistry, University of Chicago, Chicago, IL, 60637 USA*

(Dated: November 5, 2014)

The high quantum efficiency of photosynthetic complexes has inspired researchers to explore new routes to utilize this process for photovoltaic devices. Quantum coherence has been demonstrated to play a crucial role within this process. Herein, we propose a three-dipole system as a model of a new photocell type which exploits the coherence among its three dipoles. We have proved that the efficiency of such a photocell is greatly enhanced by quantum coherence. We have also predicted that the photocurrents can be enhanced by about 49.5% in such a coherent coupled dipole system compared with the uncoupled dipoles. These results suggest a promising novel design aspect of photosynthesis-mimicking photovoltaic devices.

PACS numbers: 42.50.Gy, 78.67.-n, 82.39.Jn, 84.60.Jt

I. INTRODUCTION

Long-lived quantum coherence been observed in photosynthesis after laser excitation [1–7]. It has attracted much attention on how quantum coherence could be enhanced in complex biological environment and how it may play a key role in efficient exciton transports [8–12]. It is well known that the photon-to-charge conversion quantum efficiency of photosynthesis in plants, bacteria, and algae can be almost 100% under certain conditions. While photosynthesis converts sunlight into chemical energy, solar cell converts sunlight into electric energy. According to Shockley and Queisser, the efficiency of photovoltaic energy conversion is limited to 33%, based on the energy band gap and solar spectrum, due to the radiative recombination of electron-hole pairs, thermalization, and unabsorbed photons [13]. Various attempts have been made to improve the performance of photovoltaic devices [14–18]. Mimicking photosynthesis presents a promising route by which to increase the efficiency of the current solar cell technology [19]. Consequently, there has been a long-standing and increasing interest in the understanding of the physics describing the energy conversion within photosynthesis. Recently, quantum coherence has demonstrated its crucial role in the energy conversion during photosynthesis [1–12]. Similarly, it has been shown that quantum coherence can be used to alter the conditions of the detailed balance and thereby enhance the quantum efficiency in photocell [20–23]. In principle, the Shockley-Queisser model is a two-extended-level model. By incorporating more levels and tuning them carefully, the conversion efficiency can be improved.

Recently, Creatore *et al.* [24] have shown that the delocalized quantum state is capable of improving the photocurrent of a photocell by at least 35% in compared with a photocell with the localized quantum state when treating the photon-to-charge conversion as a continuous Carnot-like cycle [25]. Within their model, the two delocalized states, called the bright and dark states, of the dipole-dipole interacting two donors play a key role in improving the efficiency of the PV cell. Due to the constructive interference, the optical transition rate between the ground and the bright states becomes two times stronger than the uncoupled donor case. While it is blocked through the bright state due to the destructive interference, the electron transition from the excited donor to the acceptor is made only through the dark state and its rate is two times larger than the uncoupled donor case, due to the constructive interference. Consequently, the presence of quantum coherence of the delocalized donor states alters the conditions for the thermodynamic detailed balance; that results in the enhancement of the efficiency of the photocell.

In this paper, we show that a photocell with three suitably arranged electron donors coupled via dipole-dipole interactions can result in an enhancement of photocurrents by about 49.5% over a classical photocell. While inspired by Creatore *et al.* [24], our three coupled donors, rather than the two coupled ones, makes another big improvement in the efficiency of a PV cell. The origin of the photocurrent enhancement is explained by the key roles of the delocalized excited states of the donor system. The dipole-dipole coupling between donors make three degenerate and localized one-exciton levels split into three delocalized levels: the bright, almost-dark, and dark states. The photon absorption and emission rates between the ground and the bright excited state becomes about 2.91 times larger than that of the uncoupled donor case, which is due to the constructive interference of three donors. While the electron transferring from the donor to the acceptor through the almost-dark state is enhanced by about 2.91 times compared to the uncoupled donor case, but is almost blocked through the bright state, which are also due to the constructive and destructive interfer-

* kais@purdue.edu

ences of the delocalized donor states. Basically, essential physics of our triple-donor model is similar to that of Creatore *et al.*'s two donor model, but more enhanced by collective properties. While it seems challenging, our proposed model could be realized by nanotechnologies inspired by natural light-harvesting structures.

II. PV MODELS WITH TWO DONORS

Before introducing a photovoltaic cell model with three donors, we discuss in detail how a configuration of two dipoles moments of two donor affects the efficiency of a PV cell in Creatore *et al.*'s model [24]. The excitation of a molecule is simply modeled as a two-level system with the ground state $|b\rangle$ and excited state $|a\rangle$. The optical transition between them is characterized by the optical dipole moment $\boldsymbol{\mu} = e\langle a|\boldsymbol{r}|b\rangle$. For a molecular aggregate composed of electric neutral molecules, the intermolecular interaction is given by the electrostatic dipole-dipole coupling [3]

$$J_{12} = \frac{1}{4\pi\epsilon\epsilon_0}\left(\frac{\boldsymbol{\mu}_1\cdot\boldsymbol{\mu}_2}{r^3} - \frac{3(\boldsymbol{\mu}_1\cdot\boldsymbol{r})(\boldsymbol{\mu}_2\cdot\boldsymbol{r})}{r^5}\right), \qquad (1)$$

where dipole moment $\boldsymbol{\mu}_1$ is located at $\boldsymbol{r}_1$, $\boldsymbol{\mu}_2$ at $\boldsymbol{r}_2$, and $\boldsymbol{r} = \boldsymbol{r}_2 - \boldsymbol{r}_1$ is the radius vector from $\boldsymbol{\mu}_1$ to $\boldsymbol{\mu}_2$. Typically, the strength of J_{12} is much weaker than the excitation energy $\hbar\omega = E_a - E_b$. The exciton dynamics of the aggregate is described by Hamiltonian [26]

$$H = \sum_i \hbar\omega_i\sigma_i^+\sigma_i^- + \sum_{i\neq j} J_{ij}(\sigma_i^-\sigma_j^+ + h.c.) \qquad (2)$$

where $\sigma^+ = |a\rangle\langle b|$ and $\sigma^- = |b\rangle\langle a|$ are the Pauli raising and lowering operators, respectively.

According to Eq. (1) the strength of J_{12} depends on how dipole moments are aligned. In Creatore *et al.*'s paper [24], the donor is a dimer where the dipole moment $\boldsymbol{\mu}_1$ is always perpendicular to the radius vector $\boldsymbol{r}$ so the second term in Eq. (1) vanishes. The dipole-dipole coupling is given by $J_{12} \propto \boldsymbol{\mu}_1\cdot\boldsymbol{\mu}_2 = \mu_1\mu_2\cos\theta$ with angle θ between two dipole moments. This gives rise to the simple angle-dependence energy gap $\Delta E = 2J_{12}^0|\cos\theta|$ between the symmetric and antisymmetric excited states. The spontaneous decay rates are also proportional to $|\mu|^2(1\pm\cos\theta)$.

Molecules in aggregates, however, are more probable to be aligned collectively, not independently. We study how the H and J aggregate donor alignments affect the efficiency of PV cells. As illustrated in Fig. 1, we consider the two dipole moments tilted at the same angle θ with respect to the vertical axis. The angle dependence of the dipole-dipole coupling of Eq. (1) becomes

$$J_{12}(\theta) = J_{12}^0\left(1 - 3\cos^2(\tfrac{\pi}{2} - \theta)\right). \qquad (3)$$

This implies the angle dependence of the Davidov energy splitting $\Delta E(\theta) = 2|J_{12}(\theta)|$ between the symmetric and antisymmetric states and explain the transition between the H-aggregate and the J-aggregate at the magic angle $\theta_c = \cos^{-1}(\frac{1}{\sqrt{3}}) \approx 54.74°$ when the angle is measured from $\boldsymbol{r}$. Here the angle is measured with respect to the vertical axis so one has the magic angle $\theta_c \approx 35.26°$ as shown in Fig. 2.

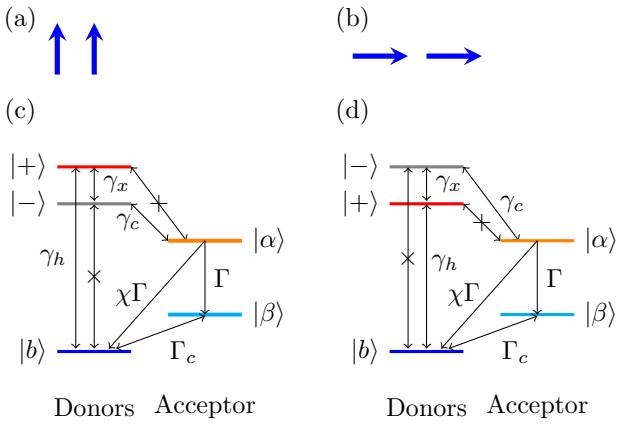

Figure 1. Alignments of two dipole moments for (a) H-aggregate and (b) J-aggregate. Energy level diagrams and electron transition paths of (c) H-aggregate and (d) J-aggregate. The symmetric state $|+\rangle$ is optically bright and has the absorption and emission rate γ_h, but has no electron transition channel to the donor. The antisymmetric state $|-\rangle$ is dark but has the electron transfer path to the donor. The electron transition rate γ_x between the bright state $|+\rangle$ and dark state $|-\rangle$ is caused by thermal phonons.

In contrast to Creatore *et al.*'s configuration, the symmetric state $|+\rangle = \frac{1}{\sqrt{2}}(|a_1\rangle + |a_2\rangle)$ in our model is always an optically active state (bright state) [27]. For angles less than θ_c, this level is higher than the antisymmetric (dark) state $|-\rangle = \frac{1}{\sqrt{2}}(|a_1\rangle - |a_2\rangle)$ so the optical transition is shifted to the blue (H-aggregate). On the other hand, for angles greater than θ_c, the antisymmetric state is higher so the optical transition is changed to the red (J-aggregate). Note that classically the total dipole moment is always $2|\mu|$ because the two dipole moments point to the same direction. The dipole matrix element between the ground and bright states is $\sqrt{2}|\mu|$ so the optical transition rate γ_h, proportional to the square of the dipole matrix element, becomes doubled, i.e, $\gamma_h = 2\gamma_{1h}$, in compared with an uncoupled donor case. We calculate how the current enhancement is dependent on the angle θ, as plotted in Fig. 2. The two energy levels $E_\pm$ for the symmetric and antisymmetric states move to $(E_a - E_b)/2$ as the angle θ increases. This affects the Bose-Einstein distributions, n_h of thermal photons, n_x and n_c of thermal phonon through the gaps $E_+ - E_b$, $E_+ - E_-$, and $E_\pm - E_\alpha$, respectively. Because of $(E_a - E_b) \gg J$, the distribution n_h is dependent little on the angle θ. However, n_x and n_c are strongly affected by the angle θ so drastic changes in current enhancement. For H-aggregate case ($\theta < \theta_c$), n_x increases but n_c decreases as angle θ increases. So the the current enhancement decreases as angle θ increases. For

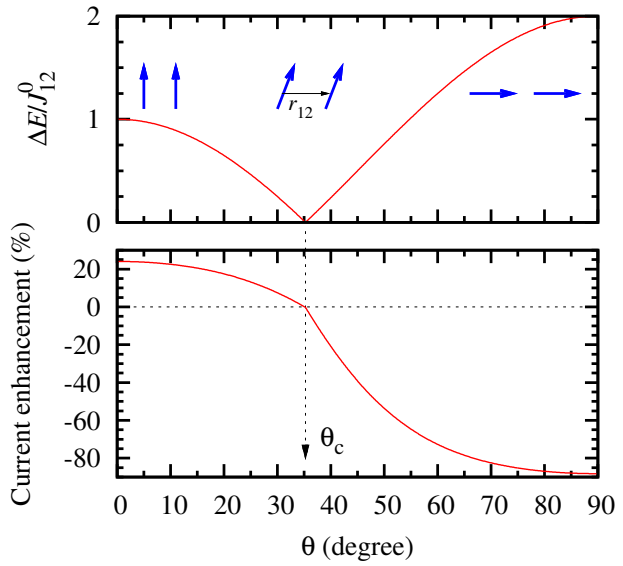

Figure 2. (a) The energy gap ΔE between the bright and dark states and (b) the current enhancement as a function of the tilt angle θ with respect to the vertical axis. In (a) the alignment of two dipole moments is shown as the blue arrows. The two parallel dipole moments are aligned in head to head manner (H-aggregate) at $\theta = 0$ and in head to tail manner (J-aggregate) at $\theta = \pi/2$. In (b) the black arrow points to the magic angle $\theta_c \approx 35.26^\circ$.

J-aggregate case ($\theta > \theta_c$), the bright state is lower than the dark state. An electron in the bright state jumps to the dark state via only the absorption γ_x of thermal phonons (in H-aggregate case, the transition from the bright to dark states can be done via the stimulated emission and spontaneous emission of thermal phonons, $\gamma_x(1+n_x)$). Thus, the transition from the donor to acceptor is very low, and the current enhancement is negative as shown in Fig. 2. In our model as well as Creatore *et al.*'s model [24], two donors are coupled to the acceptor so the bright state has no electron transferring channel to the acceptor because of the destructive interference. If a donor system is composed of many molecules (for example a linear chain), it is likely that only some donor molecules (or the molecules at the end site) are coupled to the acceptor so the transition path of the bright state to the donor would not be blocked.

III. PV MODEL WITH THREE DIPOLE DONORS

A. Model

The photocell model, proposed here, is depicted in Fig. 3. The picture of a classical cyclic engine is described as the following: D_1, D_2, and D_3 represent three identical and initially uncoupled donor molecules which are aligned around an acceptor molecule A. Initially, the system starts in the ground state $|b\rangle$. The cycle of electron transport begins with the absorption of solar photons populating the uncoupled donor excited states $|a_1\rangle$, $|a_2\rangle$, and $|a_3\rangle$. Then the excited electrons can be transferred to the acceptor molecule, the charge-separated state $|\alpha\rangle$, with any excess energy radiated as a phonon. The excited electron is then assumed to be used to perform work, leaving the charge-separated state $|\alpha\rangle$ decaying to the sub-stable state $|\beta\rangle$. The recombination between the acceptor and the donor is also considered with a decay rate of $\Gamma_{\alpha\to b} = \chi\Gamma$, where χ is a dimensionless fraction. This loss channel brings the system back into the ground state without producing a work current, which could be a significant source of inefficiency. Finally, the state $|\beta\rangle$ decays back to the charge neutral ground state, closing the cycle. If considering the quantum effects resulting from the long-range dipole-dipole interaction, the new element of the system is the formation of new optically excitable states through strong exciton coupling among the donor molecules [24].

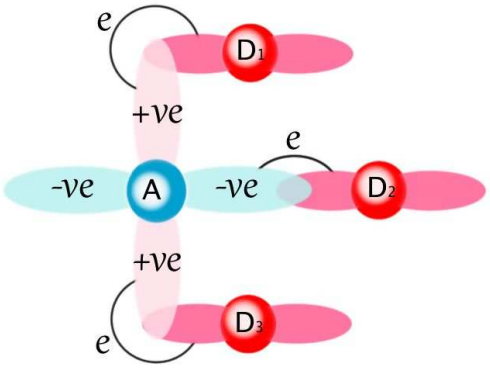

Figure 3. Schematics of our PV cell. Three optically active donors, denoted by D_1, D_2, D_3, become excited by absorbing incident photons and their excited electrons are transferred to the acceptor A. The pink and blue shadowed regions surrounding the molecules represent the molecular orbitals representing the spatial distribution of electron density.

For simplicity, we assume that three donors (D_1, D_2 and D_3) are identical and degenerate, so the uncoupled excited states $|a_1\rangle, |a_2\rangle$ and $|a_3\rangle$ of the three donors have the same excitation levels $E_1 = E_2 = E_3 = \hbar\omega$. Furthermore, their dipole moments are aligned to the same direction, $\boldsymbol{\mu}_1 = \boldsymbol{\mu}_2 = \boldsymbol{\mu}_3 = \boldsymbol{\mu}$ as depicted in Fig. 3. We assume the dipole-dipole interaction between only nearest neighbors. The dipole-dipole couplings between D_1 and D_2, and D_2 and D_3 are denoted by J, but there is no coupling between D_1 and D_3. The Hamiltonian for the system of three interacting donors is written as

$$H = \sum_{i=1}^{3} \hbar\omega\sigma_i^+\sigma_i^- + J(\sigma_1^-\sigma_2^+ + \sigma_2^-\sigma_3^+ + h.c.)\,. \qquad (4)$$

It is straightforward to obtain the three single-excitation

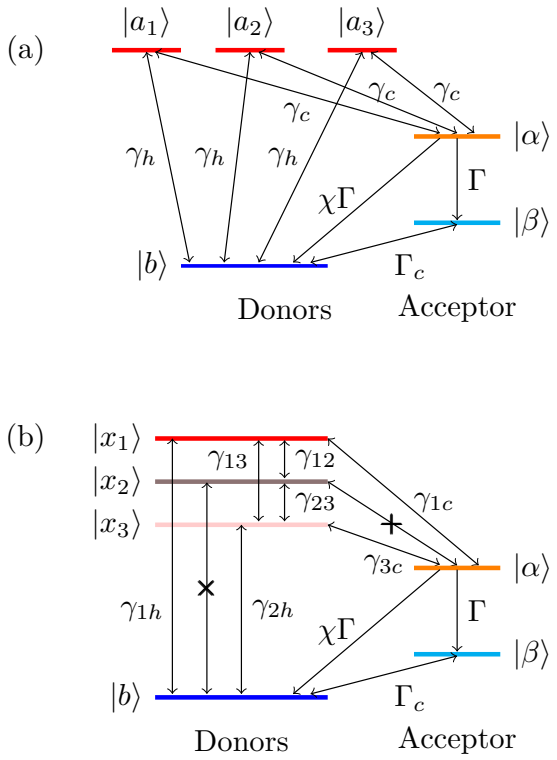

Figure 4. Energy levels of the PV models (a) with the acceptor and three uncoupled donors and (b) with the acceptor and three dipole-dipole coupled donors. Black arrows indicate possible electron-transition paths. In (a) all the three donors are uncoupled and identical so have the same excitation energies (E_i), the same the photon absorption and emission rates γ_h between the ground state $|b\rangle$ and excited states $|a_i\rangle$, and the same electron transfer rates γ_c between the excited donors ($|a_i\rangle$) and the acceptor ($|\alpha\rangle$). In (b) due to the dipole-dipole couplings between three donors, the three degenerate excited levels in (a) become split, denoted by $|x_i\rangle$. The dark level ($|x_2\rangle$) is optically forbidden and has no electron transfer path to the donor ($|\alpha\rangle$).

states of Hamiltonian (4): $|x_1\rangle = \frac{1}{2}(|a_1\rangle + \sqrt{2}\,|a_2\rangle + |a_3\rangle)$, $|x_2\rangle = \frac{1}{\sqrt{2}}(|a_1\rangle - |a_3\rangle)$, and $|x_3\rangle = \frac{1}{2}(|a_1\rangle - \sqrt{2}\,|a_2\rangle + |a_3\rangle)$. The corresponding eigenvalues are obtained as $E_{x_1} = E + \sqrt{2}J, E_{x_2} = E$, and $E_{x_3} = E - \sqrt{2}J$.

The dipole moment between the state $|x_1\rangle\,/\,|x_3\rangle$ and the ground state $|0\rangle$ is enhanced/weakened by constructive interference between the individual transition dipole matrix elements, $\mu_{x_1/x_3} = \frac{1}{2}(\mu_1 \pm \sqrt{2}\mu_2 + \mu_3) = (1 \pm \frac{1}{\sqrt{2}})\mu$, while the dipole moment of the state $|x_2\rangle$ cancels due to destructive interference. This means the state $|x_2\rangle$, comprised of the antisymmetric combination of the uncoupled $|a_1\rangle$ and $|a_3\rangle$ states, describes an optically forbidden dark state. On the contrary, the $|x_1\rangle$ and $|x_3\rangle$ states describe two optically active bright states with photon absorption and emission rates $\gamma_{1h} \propto |\mu_{x_1}|^2 = (\frac{3}{2} + \sqrt{2})|\mu|^2$ and $\gamma_{3h} \propto |\mu_{x_3}|^2 = (\frac{3}{2} - \sqrt{2})|\mu|^2$, respectively, in compared with the uncoupled case, $\gamma_h \propto |\mu|^2$. In other words, $|x_1\rangle$ is much brighter than $|x_3\rangle$, as the photon absorption and emission rate of $|x_1\rangle$ is enhanced while that of $|x_3\rangle$ is weakened. Obviously, the dark state $|x_2\rangle$ has a resultant charge transfer matrix element equal to zero.

The intermolecular dipole interaction will also modify the transition rate between the donors and acceptor. The electron transfer matrix elements leading to charge separation have been chosen to have the same magnitudes $|t_{D_1A}| = |t_{D_2A}| = |t_{D_3A}| = t$. Also, we assume that the acceptor molecule hosts an electron within its lowest unoccupied molecular orbital, which is characterized by the shape of the d-orbitals (See Fig. 3). We have also assumed that the donor molecules are located close to different lobes of the acceptor molecular orbital; this leads to electron transfer matrix elements with the same magnitudes but different signs, i.e., $t_{D_1A} = -t_{D_2A} = t_{D_3A} = t$. Due to effects of the dipole-dipole interactions, the eigenstates of the three optically excited donors are no longer uncoupled, but are coherent exciton states. The bright states $|x_1\rangle\,/\,|x_3\rangle$ have matrix elements $t_{x_1A/x_3A} = \frac{1}{2}(t_{D_1A} \mp \sqrt{2}t_{D_2A} + t_{D_3A}) = (1 \mp \frac{1}{\sqrt{2}})t$, giving decreased/enhanced electron transfer rates of $\gamma_{1c/3c} \propto |t_{x_1A/x_3A}|^2 = (\frac{3}{2} \mp \sqrt{2})|t|^2$, in compared with the uncoupled case $\gamma_c \propto |t|^2$. These modifications of electron transfer matrix elements play a crucial role in the enhancement of photocurrents within our photocell model. The assumptions surrounding the electron transfer matrix elements is identical to that in Ref. 24.

Another crucial procedure in our model is phonon-mediated energy relaxation, which can be very effective between exciton states with strong pigment overlap [24, 28]. These relaxations are included in our kinetic model via the relaxation rates $\gamma_{12}, \gamma_{13}, \gamma_{23}$. Assuming that the new donor states are directly populated by the absorption of weak incoherent solar photons, the kinetics of the optically excited states obey the Pauli master equation (PME) by treating the donor-light, electron transfer, and bright-dark relaxation coupling by second-order perturbations [24].

The PMEs for the uncoupled case, describing the processes as shown in Fig. 4 (a), are written as

$$\begin{aligned}
\dot{p}_1 &= \gamma_h[n_h p_b - (1+n_h)p_1] + \gamma_c[n_c p_\alpha - (1+n_c)p_1],\\
\dot{p}_2 &= \gamma_h[n_h p_b - (1+n_h)p_2] + \gamma_c[n_c p_\alpha - (1+n_c)p_2],\\
\dot{p}_3 &= \gamma_h[n_h p_b - (1+n_h)p_3] + \gamma_c[n_c p_\alpha - (1+n_c)p_3],\\
\dot{p}_\alpha &= \gamma_c(1+n_c)(p_1+p_2+p_3) - 3\gamma_c n_c p_\alpha - \Gamma(1+\chi)p_\alpha,\\
\dot{p}_\beta &= \Gamma_c[N_c p_b - (1+N_c)p_\beta] + \Gamma p_\alpha
\end{aligned} \tag{5}$$

where we use the notation $p_i = \rho_{i,i}$ with indices i running as $b, 1 = a_1, 2 = a_2, 3 = a_3, \alpha, \beta$. Similarly, the PMEs for the dipole-dipole coupled case, whose processes are shown in Fig. 4 (b), are given by

$$\begin{aligned}
\dot{p}_1 &= \gamma_{1h}[n_{1h}p_b - (1+n_{1h})p_1] + \gamma_{12}[n_{12}p_2 - (1+n_{12})p_1] + \gamma_{13}[n_{13}p_3 - (1+n_{13})p_1] + \gamma_{1c}[n_{1c}p_\alpha - (1+n_{1c})p_1],\\
\dot{p}_2 &= \gamma_{12}[(1+n_{12})p_1 - n_{12}p_2] + \gamma_{23}[n_{23}p_3 - (1+n_{23})p_2],\\
\dot{p}_3 &= \gamma_{3h}[n_{3h}p_b - (1+n_{3h})p_3] + \gamma_{23}[(1+n_{23})p_2 - n_{23}p_3] + \gamma_{13}[(1+n_{13})p_1 - n_{13}p_3] + \gamma_{3c}[n_{3c}p_\alpha - (1+n_{3c})p_3],\\
\dot{p}_\alpha &= \gamma_{1c}[(1+n_{1c})p_1 - n_{1c}p_\alpha] + \gamma_{3c}[(1+n_{3c})p_3 - n_{3c}p_\alpha] - \Gamma(1+\chi)p_\alpha,\\
\dot{p}_\beta &= \Gamma p_\alpha + \Gamma_c[N_c p_b - (1+N_c)p_\beta],
\end{aligned} \tag{6}$$

where index i of p_i runs as $b, 1 = x_1, 2 = x_2, 3 = x_3, \alpha, \beta$. In Eqs. (5) and (6), the equation of motion for $p_b = \rho_{bb}$ is determined by the conservation of the probability, $\sum_i p_i = \sum_i \rho_{ii} = 1$. In Eqs. (5) and (6), n_h and n_{1h} (n_{3h}) stand for the average numbers of photons with frequencies matching the transition energies from the ground state $|b\rangle$ to the excited states $|a_i\rangle$ and $|x_1\rangle$ ($|x_3\rangle$), respectively. n_c and n_{1c} (n_{3c}) are the thermal occupation numbers of ambient phonons at room temperature, $T_a = 300$ K, with energies $E - E_\alpha$ in Eq. (5) and $E_{x_1} - E_\alpha$ ($E_{x_3} - E_\alpha$) in Eq. (6). n_{12}, n_{13}, and n_{23} represent the corresponding thermal occupations at T_a with energies $E_{x_1} - E_{x_2}$, $E_{x_1} - E_{x_3}$, and $E_{x_2} - E_{x_3}$, respectively. N_c is the corresponding thermal occupation at T_a with the energy $E_\beta - E_b$. The rates in Eqs. (5) and (6) obey local detailed balance and correctly lead to a Boltzmann distribution for the level population if the thermal averages for the photon and phonon reservoirs are set to a common temperature, such as room temperature. We consider the initial condition to be a fully occupied ground state, i.e., $\rho_{bb}(t=0) = 1$.

B. Results

To calculate the population of each state, we use the following parameters: the energy levels are $E - E_b = 1.8$ eV, $E - E_\alpha = E_\beta - E_b = 0.2$ eV, $J_{12} = J_{23} = J = 0.015$ eV; the transfer rates are $\gamma_h = 0.62 \times 10^{-6}$ eV, $\gamma_c = 6$ meV, $\Gamma = 0.12$ eV, $\Gamma_c = 0.025$ eV [20, 23, 24]. We assume that the superposition states are stable under the steady-state operation, so that $\gamma_{13}, \gamma_{12}, \gamma_{23}$ have to satisfy the relationship: $\gamma_{13} = 2\gamma_{12} = 2\gamma_{23} \leq 2\sqrt{2}J$ [29]. Here, we choose as a limiting condition: $\gamma_{13} = 2\gamma_{12} = 2\gamma_{23} = 2\sqrt{2}J$. We also employed this as a limiting condition for Creator's model, to create an appropriate comparison with our model. Figs. 5 (a) and (b) show the populations of each state in the absence and presence of coupling. Due to the dipolar interaction among donors, the populations of the donors' ground state, $|b\rangle$, is significantly decreased while the populations of the acceptors' states, $|\alpha\rangle$ and $|\beta\rangle$, are notably increased in the presence of coherence when the system reaches the steady-state operation. These changes are responsible for the enhanced photocurrents.

Taking a modest recombination rate $\Gamma_{a\to b} = \chi\Gamma$ with $\chi = 20\%$, Fig. 6 shows the current enhancement as a function of the transition rate, γ_c, using the other parameters listed before. Under the upper limit condition, when $\gamma_c = \gamma_{12} = \gamma_{23}$, there is no current enhancement. This means that the charge transfer via the channels $|x_1\rangle \to |\alpha\rangle$, $|x_1\rangle \to |x_3\rangle \to |\alpha\rangle$, and $|x_1\rangle \to |x_2\rangle \to |x_3\rangle \to |\alpha\rangle$ are as fast as the combined transfer through the independent channels $|a_1\rangle \to |\alpha\rangle$, $|a_2\rangle \to |\alpha\rangle$, and $|a_3\rangle \to |\alpha\rangle$. However, when $\gamma_c < \gamma_{12} = \gamma_{23}$, the coherent coupling leads to substantial current enhancements when compared to the configuration without coupling. Fig. 6 also shows that the current enhancement may reach as high as 49.5%, comparing this with 35% in Creator's model. This can be explained by two factors: (i) the optical transition rate between the ground and the bright state is enhanced from 2 times to 2.9 times. (ii) the electron transition from the almost-dark (dark state in Ref. [24]) to acceptor is increased from 2 times to 2.9 times. So a simple calculation shows the enhancement of PV model, $49.5\% \approx \frac{2.9}{2} \times 35\%$.

We have also explored the effect of the recombination rate, $\Gamma_{a\to b} = \chi\Gamma$, on the current enhancement. In Fig. 7,

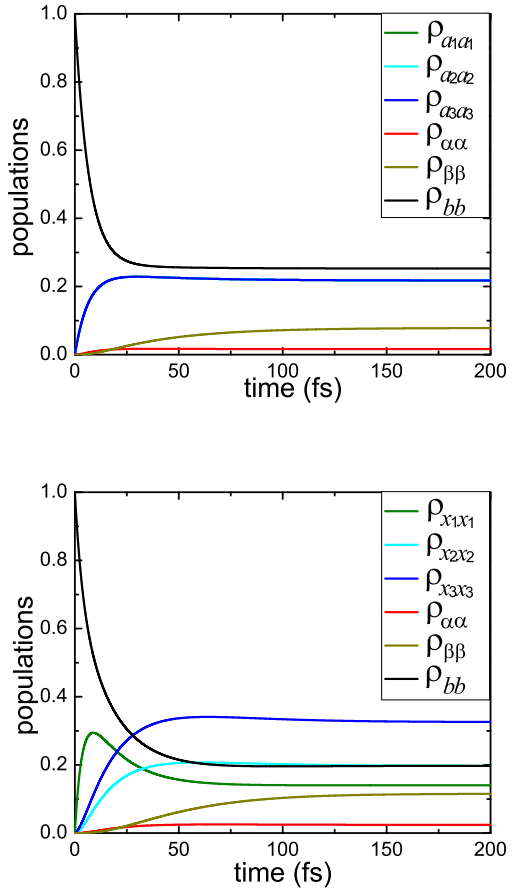

Figure 5. (a) The time-evolutions of the populations p_i of the levels from the numerical solution of the Pauli master equation (Eq. 5) for uncoupled donors. (b) Numerical solutions of the Pauli master equation (Eq. 6) for coupled donors.

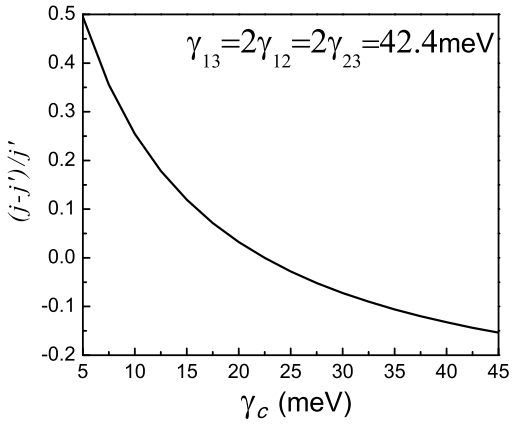

Figure 6. Relative current enhancement $(j-j')/j'$ as a function of the transition rate γ_c between the donors and acceptor. Using the upper limit condition for γ_{12}, γ_{23}, and γ_{13}, we can get a current enhancement as high as 49.5%. On the other hand when $\gamma_c = \gamma_{12} = \gamma_{23}$, there is no current enhancement.

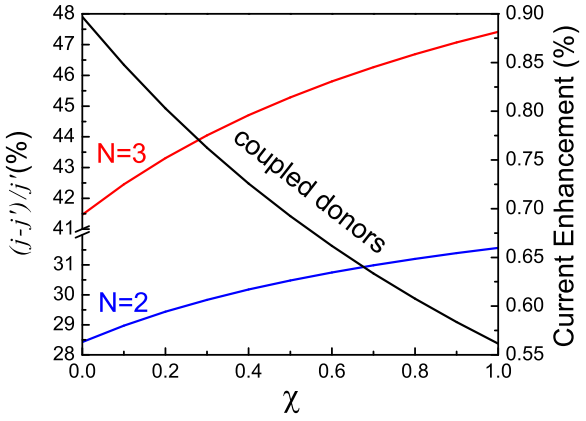

Figure 7. Relative current enhancement $(j-j')/j'$ as a function of the recombination rate χ using $\gamma_c = 6$ meV. j and j' are the electric current in the excitonically coupled and uncoupled cases, respectively, when the system reaches steady-state operation. The red line represents the current enhancement for the system with three donors; the blue line represents the current enhancement for the system with two donors proposed by Creator *et al.*; the black line represents the current enhancement of our model comparing to Creator's model in the presence of dipolar coupling.

we show not only the current enhancement for the system comprised of three donors, (which is proposed here,) but also the current enhancement for the system with two donors, (that proposed in Ref. 24,) under similar electron transfer rate conditions. The results show that although the overall current is lower for faster recombination, the relative enhancement of the photocurrent is actually slightly larger for strong recombination. This behavior is analogous to that in the system with two donors [24]. From Fig. 7, we also notice that the current enhancement in our three-donor system is much larger than that in Creatore's two-donor system at any value for the recombination rates. However, the current enhancement, on the order of 10^{-3}, from the two-coupled-donor model to the three-coupled-donor model is very small.

Within this scheme, we assume there to be a *load* connecting the acceptor levels α and β. According to Fermi-Dirac statistics, the voltage, V, across this load can be expressed as $eV = E_\alpha - E_\beta + k_B T_a \log(\rho_{\alpha\alpha}/\rho_{\beta\beta})$, where e is the fundamental charge of the electron [20, 24]. Thus, we can assess the performance of our proposed photocell in terms of its photovoltaic properties. The steady-state current-voltage $(j-V)$ characteristic and power generated are shown in Fig. 8. The current and voltage are evaluated using the steady-state solutions of the PMEs; the calculations are performed at increasing rate Γ as other parameters are fixed, from open circuit regime where $j \to 0$ ($\Gamma \to 0$) to the short circuit regime where $V \to 0$. The power, P, is evaluated by the formula $P = j \cdot V$. In Fig. 8, the peak current enhance-

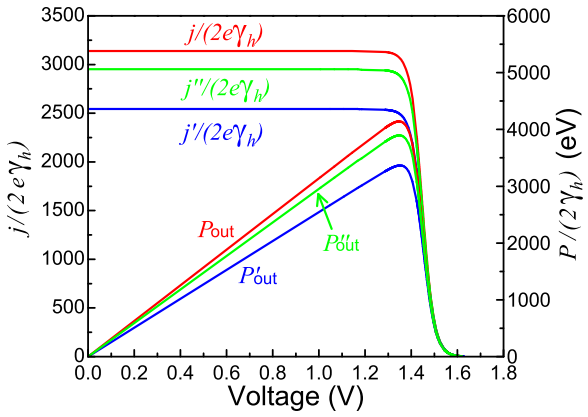

Figure 8. Current and power generated as a function of the induced cell voltage, V, at room temperature. The blue lines represent the dimensionless current ($j'/(2e\gamma_h)$) and power generated (P'_{out}) of the system with three uncoupled dipoles ($J_{12} = J_{23} = J_{13} = 0$); the red lines represent the dimensionless current ($j/(2e\gamma_h)$) and power generated (P_{out}) of the system with three coupled dipoles ($J_{12} = J_{23} \neq 0, J_{13} = 0$); the green lines represent the dimensionless current ($j''/(2e\gamma_h)$) and power generated (P''_{out}) of the system with two coupled dipoles, which is proposed in Ref. 24.

ment is roughly 23.4% in uncoupled three-donor system ($J_{12} = J_{23} = J_{13} = 0$) relative to the coupled three-donor system ($J_{12} = J_{23} \neq 0, J_{13} = 0$). Following the definition contained in Ref. [24], the peak delivered power enhancement is about 23.0% in the uncoupled three-donor system ($J_{12} = J_{23} = J_{13} = 0$) relative to the coupled three-donor system ($J_{12} = J_{23} \neq 0, J_{13} = 0$). We also show in Fig. 8 that the current-voltage characteristic and power generated for the system with two coherent donors, proposed in Ref. [24]. From these results, we find that when compared to the two coherent donor system, the three coherent donor system has an enhancement of 6.3% in both peak current and peak delivered power.

IV. CONCLUSION

The study of photosynthesis has inspired a new method by which we may harness quantum effects and coherent coupling amongst chromophores for the formation of coherent superposition to realize an artificial light-harvesting system at the molecular scale. In this paper, we propose a simple model to improve the performance of a theoretical photocell system. With suitably arranged electron donors, the photocurrents and power can be greatly enhanced through harnessing quantum effects.

The studied system is a photocell where the excitations are assumed resonant; for solar cells the excitation is done by solar radiation which has broad spectrum. However, the presented approach can be utilized in solar cells in different ways. One approach is to extend the system into N-dipole (extended bands) and use solar radiation for excitation. Another possibility is to host the dipole aggregates in solar cell materials close to the LUMO to suppress recombination and hence increase the collected photogenerated carriers [30].

Developing new concepts to harvest and utilize energy based on lessons learned from nature like those in photosynthesis is of great current interest. Examining the current-voltage characteristic and power generated for the system with three coherent dipoles, we have found an efficiency enhancement of about 6.3% compared with two coherent dipoles. This encouraging trend suggest a promising novel design aspect of photosynthesis-mimicking photovoltaic devices.

[1] G.S. Engel, T.R. Calhoun, E.L. Read, T.-K. Ahn, T. Mančal, Y.-C. Cheng, R.E. Blankenship, and G.R. Fleming, *Evidence for wavelike energy transfer through quantum coherence in photosynthetic systems*, Nature **466**, 782 (2007).

[2] T.R. Calhoun, N.S. Ginsberg, G.S. Schlau-Cohen, Y.C. Cheng, M. Ballottari, R. Bassi, and G.R. Fleming, *Quantum Coherence Enabled Determination of the Energy Landscape in Light-Harvesting Complex II*, J. Phys. Chem. B, **113**, 16291 (2009).

[3] D. Abramavicious, B. Palmieri, and S. Mukamel, *Extracting single and two-exciton couplings in photosynthetic complexes by coherent two-dimensional electronic spectra*, Chem. Phys. **357**, 79 (2009).

[4] G. Panitchayangkoon, D. Hayes, K.A. Fransted, J.R. Caram, E. Harel, J. Wen, R.E. Blankenship, and G.S. Engel, *Long-lived quantum coherence in photosynthetic complexes at physiological temperature*, PNAS, **107**, 12766, (2010).

[5] E. Harel, A.F. Fidler, and G.S. Engel, *Real-time Mapping of Electronic Structure with Single-shot Two-dimensional Electronic Spectroscopy* Proc. Natl. Acad. Sci. USA, **107**, 16444 (2010).

[6] D. Hayes, G.B. Griffin, and G.S. Engel, *Engineering coherence among excited states in synthetic heterodimer systems*, Science, **340**, 1431 (2013).

[7] E. Romero, R. Augulis, V.I. Novoderezhkin, M. Ferretti, J. Thieme, D. Zigmantas, and R. van Grondelle, *Quantum coherence in photosynthesis for efficient solar-energy conversion*, Nat. Phys. **10**, 676 (2014).

[8] M. Mohseni, P. Rebentrost, S. Lloyd, and A. Aspuru-Guzik, *Environment-assisted quantum walks in photosynthetic energy transfer*, J. Chem. Phys., **129**, 174106 (2008).

[9] M.B. Plenio, and S.F. Huelga, *Dephasing-assisted transport: quantum networks and biomolecules*, New J. Phys.,

10, 113019 (2008).

[10] P. Rebentrost, M. Mohseni, I. Kassal, S. Lloyd, and A. Aspuru-Guzik, *Environment-assisted quantum transport*, New J. Phys. **11** 033003 (2009).

[11] J. Zhu and S. Kais, *Modified scaled hierarchical equation of motion Approach for the study of quantum coherence in photosynthetic complexes*, J. Phys. Chem. B, **115**, 1531 (2011).

[12] S.-H. Yeh and S. Kais, *Population and coherence dynamics in light harvesting complex II (LH2)*, J. Chem. Phys. **137**, 084110 (2012).

[13] W. Shockley and H.J. Queisser, *Detailed Balance Limit of Efficiency of p-n Junction Solar Cells*, J. Appl. Phys., **32**, 510, (1961).

[14] P. Würfel, *Physics of Solar Cells* (Wiley-VCH, Berlin, 2009).

[15] *Quantum Efficiency in Complex Systems, Part II: From Molecular Aggregates to Organic Solar Cells* edited by U. Würfel, M. Thorwart, and, E. R. Weber, Semiconductors and Semimetals, Vol. 85 (Academic Press, San Diego, 2011).

[16] O.D. Miller, E. Yablonovitch, and S.R. Kurtz, *Strong Internal and External Luminescence as Solar Cells Approach the Shockley-Queisser Limit*, IEEE J. Photovoltaics, **2**, 303 (2012).

[17] F.H. Alharbi, *Carrier multiplication applicability for photovoltaics; a critical analysis*, J. Phys. D **46**, 125102 (2013).

[18] F.H. Alharbi and S. Kais, *Theoretical Limits of Photovoltaics Efficiency and Possible Improvements by Intuitive Approaches Learned from Photosynthesis and Quantum Coherence*, Renew. Sust. Energ. Rev. (in press); arXiv:1402.1923.

[19] R.E. Blankenship, D.M. Tiede, J. Barber, G.W. Brudvig, G. Fleming, M. Ghirardi, M.R. Gunner, W. Junge, D.M. Kramer, A. Melis, T.A. Moore, C.C. Moser, D.G. Nocera, A.J. Nozik, D.R. Ort, W.W. Parson, R.C. Prince, and R.T. Sayre, *Comparing photosynthetic and photovoltaic efficiencies and recognizing the potential for improvement*, Science **332** 811 (2011).

[20] M.O. Scully, *Quantum Photocell: Using Quantum Coherence to Reduce Radiative Recombination and Increase Efficiency*, Phys. Rev. Lett., **104**, 207701, (2010).

[21] M.O. Scully, K.R. Chapin, K.E. Dorfman, M.B. Kim, and A. Svidzinsky, *Quantum heat engine power can be increased by noise-induced coherence*, Proc. Natl. Acad. Sci. USA, **108**, 15097 (2011).

[22] A.A. Svidzinsky, K.E. Dorfman, and M.O. Scully, *Enhancing photovoltaic power by Fano-induced coherence*, Phys. Rev. A, **84**, 053818, (2011).

[23] K.E. Dorfman, D.V. Voronine, S. Mukamel, and M.O. Scully, *Photosynthetic reaction center as a quantum heat engine*, Proc. Natl. Acad. Sci. USA, **110**, 2746, (2013).

[24] C. Creatore, M.A. Parker, S. Emmott, and A.W. Chin, *Efficient biologically inspired photocell enhanced by delocalized quantum states*, Phys. Rev. Lett., **111**, 253601, (2013).

[25] It should be noted that this efficiency may not be analogous to the Shockley Quisser limit [13].

[26] The Hamiltonian (2) is identical to an XY spin Hamiltonian. One exciton state corresponds to the one spin flipped state.

[27] The single exciton eigenstates of Hamiltonian (2) are given explicitly as $|\pm\rangle = \frac{1}{\sqrt{2}}(|a_1 b_2\rangle \pm |b_1 a_2\rangle)$. For simplicity, these are written as $|\pm\rangle = \frac{1}{\sqrt{2}}(|a_1\rangle \pm |a_2\rangle)$.

[28] H. van Amerongen, L. Valkunas, and R. van Grondelle, *Photosynthetic Excitons* (World Scientific, Singapore, 2000).

[29] A. Shnirman, Y. Makhlin, and G. Schön, *Noise and Decoherence in Quantum Two-Level Systems*,

[30] S.K. Saikin, A. Eisfeld , S. Valleau, and A. Aspuru-Guzik, *Photonics meets excitonics: natural and artificial molecular aggregates*, Nanophotonics **2** 21 (2013).